

Pseudo-prospective earthquakes forecasting experiment in Italy based on temporal variation of the b-value of the Gutenberg-Richter law.

E. Biondini¹, F. D’Orazio¹, B. Lolli^{2,1} and P. Gasperini^{1,2}¹Dipartimento di Fisica e Astronomia, Università di Bologna, Bologna, I-40127, Italy. E-mail: emanuele.biondini2@unibo.it;

flavia.dorazio@studio.unibo.it; paolo.gasperini@unibo.it

²Istituto Nazionale di Geofisica e Vulcanologia, Sezione di Bologna, Italy. E-mail: barbara.lolli@ingv.it**1-Abstract**

The analysis of spatio-temporal variations of the **b-value** of the frequency-magnitude distribution (Gutenberg and Richter, 1944) of earthquake occurrence can be considered an important indicator for understanding the processes preceding strong seismic events. Indeed, this parameter is **inversely correlated** to the accumulation of differential stress in crustal rocks (Scholz, 1968).

Variations in the **b-value** can therefore provide **valuable information** about the state of stress and the probability of earthquakes occurring in a specific geographic region. Such **spatio-temporal variations** can then be analyzed as a **precursor signal** of strong seismic events. In fact, in many cases, the **b-value tends to decrease** in the preparatory stages of a strong earthquake, and then suddenly increase after the main shock has occurred (Gulia et al., 2018).

To evaluate this hypothesis, an **alarm-based** forecasting **method** using spatio-temporal variations of the b-value as a **precursor signal (b-model)** is implemented in this work.

The **forecasting capabilities** were assessed using tests and statistics specific to **alarm-based models**. These capabilities were then compared with those of the **FORE model** (Gasperini et al., 2021), which uses the occurrence of potential strong foreshocks as a precursor signal, and with those of an **ETAS-SVP model** (Biondini et al., 2023), both applied using an alarm-based approach.

Moreover, we explored both the union (**United model**) and intersection (**Inter model**) of the b-value and FORE models to analyze the combined forecasting performance.

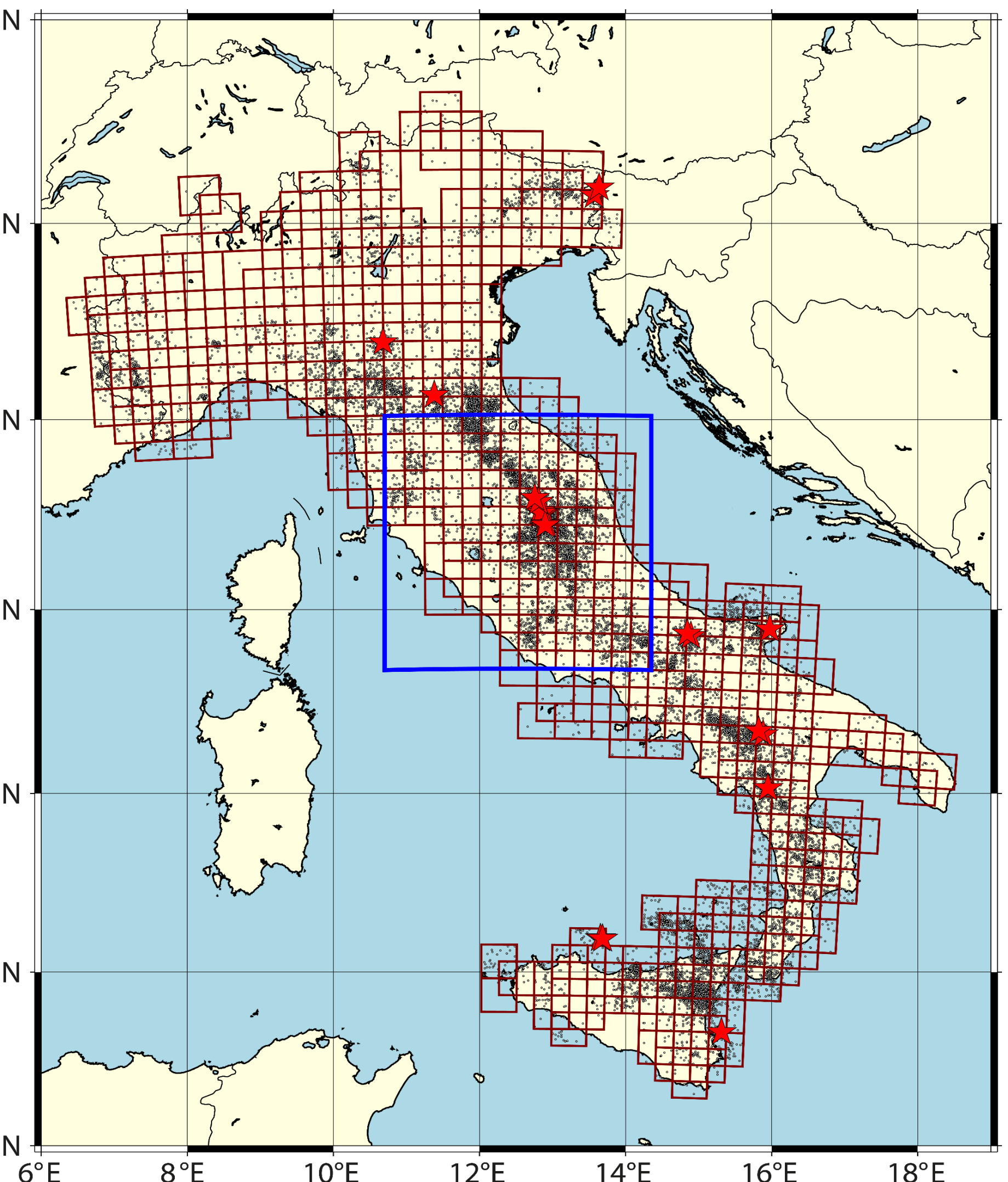


Fig. 1: Tessellation of the Italian territory region used for the models fitting and optimization. The red squared and overlapped cells represent the analysis region used for the learning period 1990-2004. The blue square represent the region adopted for the test period 2005-2022. The red stars represent the target earthquakes with $M \geq 5.0$ occurred within the Italian geographical region. Black dots show the seismicity.

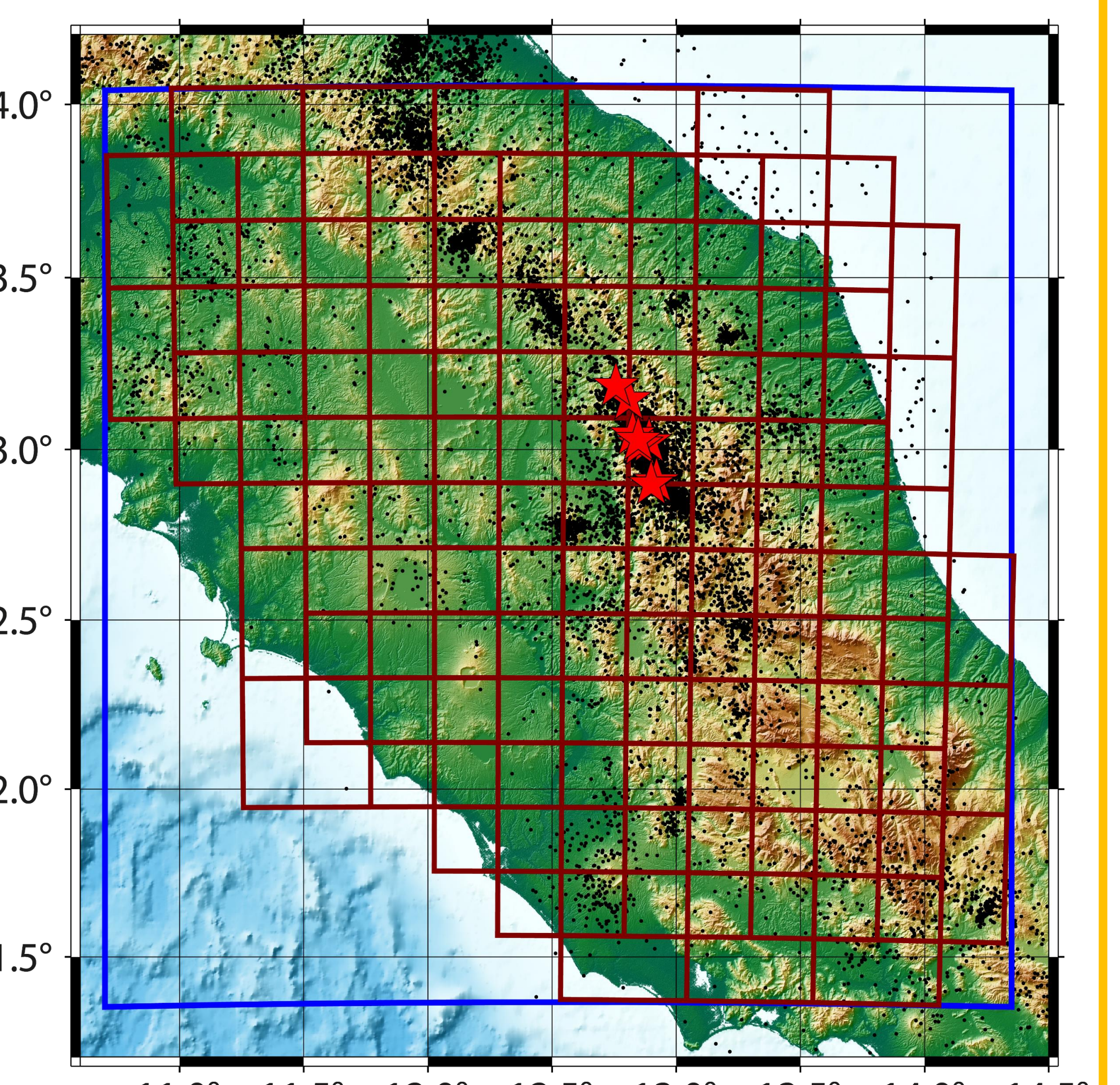


Fig. 3: Same as Fig. 1 but showing details for the Central Italy region used as test area for the pseudo-prospective forecasting experiment.

2-Setting up the forecasting experiment

- All models are fitted to forecast **earthquakes** with magnitude $Mw \geq 5.0$ in the Italian geographical region, over a **spatial grid** of 337 overlapped squared cells of side $L=30\sqrt{2}$ km shown in Fig. 1.
- The **optimization** of the different precursor signals (see Table 1) has been conducted for the period 1990-2004.
- The used **dataset** is the Homogenized instRumental Seismic (HORUS) catalog (Lolli et al. 2020) from 1960 to 2022 (downloadable from <http://horus.bo.ingv.it>).

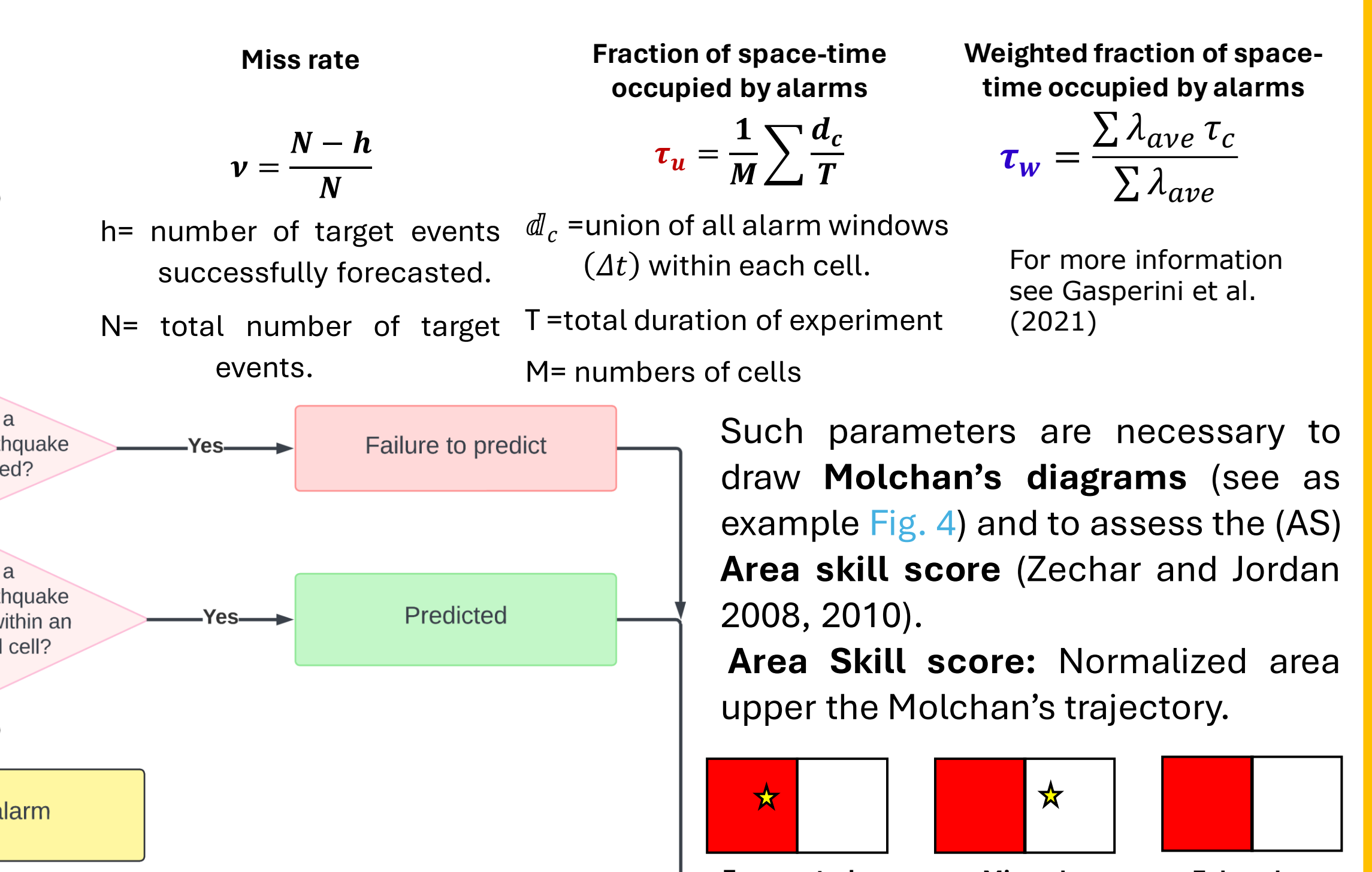
Table 1: Summary of tested forecasting models.

Model	Precursor	Reference
b-model	Decrease of the b-value below a certain threshold value.	Biondini et al., (in preparation)
FORE	Occurrence of a strong potential foreshock.	Gasperini et al., (2021)
United model	Decrease of b-value or occurrence of a potential foreshock.	Biondini et al., (in preparation)
Inter model	Decrease of b-value concurrently with an occurrence of a potential foreshock.	Biondini et al., (in preparation)
ETAS-SVP	Exceeding the expected rate of an established threshold.	Biondini et al., (2023)

3-Alarm-based approach

The alarm-based approach in **earthquake forecasting** is based on the **detection of precursor phenomena** that could indicate an **impending earthquake**. When one of these signals is detected, an **alarm** is triggered for that area. If in an alarmed area a **target earthquake** occurs it is considered as “**predicted**”.

Following Molchan (1990, 1991), the forecasting experiment is repeated many times using wider alarm durations Δt . For each Δt we estimate:



- References
- Biondini, E., D. A. Rhodes, and P. Gasperini (2023), Application of the EEP earthquake forecasting model to Italy, *Geophysical Journal International*, ggad123, doi:10.1093/gji/ggad123.
- Gasperini, P., E. Biondini, B. Lolli, A. Petrucci, and G. Vannucci (2021), Retrospective short-term forecasting experiment in Italy based on the occurrence of strong (fore) shocks, *Geophysical Journal International* 225, no. 2, 1192–1206, doi:10.1093/gji/gga592.
- Gulia, L., A. P. Rinaldi, T. Tornam, G. Vannucci, B. Enescu, and S. Wiemer (2018), The Effect of a Mainshock on the Size Distribution of the Aftershocks, *Geophysical Research Letters* 45, no. 24, doi:10.1029/2018GL080619.
- Gutenberg, B., and C. F. Richter (1944), Frequency of earthquakes in California, *Bulletin of the Seismological Society of America* 34, no. 4, 185–188, doi:10.1785/BSSA0340040185.
- Molchan, G. M. (1990), Structure of optimal strategies in earthquake prediction, *Tectonophysics* 193, no. 4, 267–275, doi:10.1016/0040-1951(91)90336-Q.
- Shebalin, P., C. Narteau, M. Holzschneider, and D. Schorrer (2011), Parametric Catalogue of Italian Earthquakes (CPTI11), version 4.0, Istituto Nazionale di Geofisica e Vulcanologia (INGV), doi:10.13127/ICPTI/CPTI11.4.
- Scholz, C. H. (1968), The frequency-magnitude relation of microfracturing in rock and its relation to earthquakes, *Bulletin of the Seismological Society of America* 58, no. 1, 399–415, doi:10.1785/BSSA0580010399.
- Zechar, J. D., and T. H. Jordan (2008), Testing alarm-based earthquake predictions, *Geophysical Journal International* 172, no. 2, 715–724, doi:10.1111/j.1365-246X.2007.03678.x.
- Zechar, J. D., and T. H. Jordan (2010), The Area Skill Score Statistic for Evaluating Earthquake Predictability Experiments, *Pure Appl. Geophys.* 167, no. 8–9, 893–906, doi:10.1007/s00024-010-0086-0.

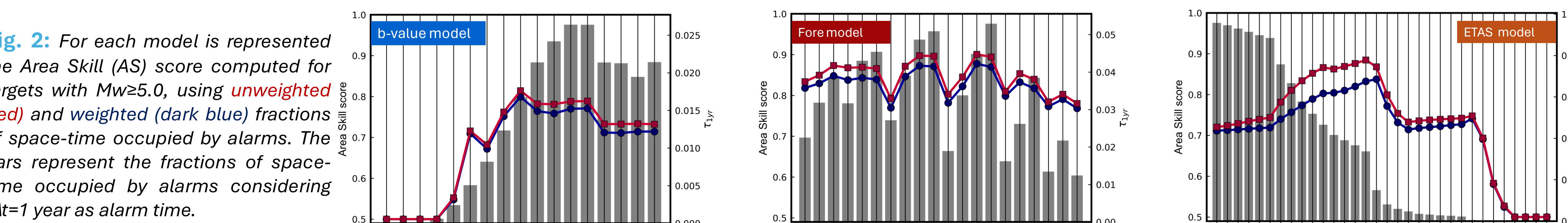


Photography encouraged

Poster

4-Optimization of alarm thresholds (Learning period)

- The **alarm threshold** for the **precursor signal** of each model was chosen through an **optimization procedure** conducted during the **learning period** (1990-2004) by testing different thresholds.
- To choose the **optimal precursors thresholds** (Fig. 2) we used the maximum **Area Skill score (AS)**.

**5-Pseudo-prospective test for the Central Italy region**

- Using the **calibrated models**, we assessed their **pseudo-prospective performance** for the **Central Italy region** indicated by the blue square in Fig. 1 and showed in detail in the Fig. 3, for the period 2005-2022.
- To assess the forecasting performance of alarm-based models we adopted the **Molchan’s diagram** (Molchan, 1990, 1991).
- Molchan’s test **compare the forecasting performance** obtained by a **forecasting method** (blue and red trajectories in the diagrams) **with** that obtained by a **purely random model** that simply forecast earthquakes in proportion to the fraction of space-time occupied by the alarms (diagonal line of the diagram).
- According to this test, the closer the **Molchan trajectory** is to the **lower left-hand corner** of the diagram, the **higher** the **performance** of the model (Fig. 4).

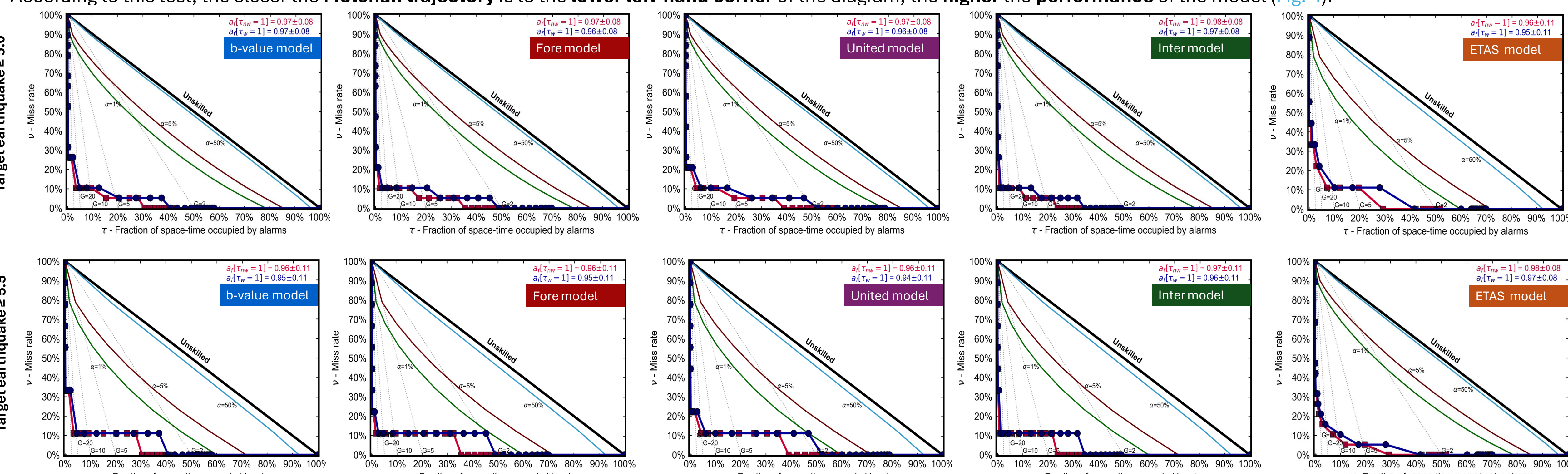


Fig. 4: Molchan diagrams and AS score of the tested models. Red and dark blue lines indicate the forecasting performance of expected daily rate threshold for unweighted (τ_u) and weighted (τ_w) fractions of space-time occupied by alarms respectively. The black continuous line indicates a purely random forecasting method that separates skilled (below the line) from unskilled (above) forecasting methods. The light blue, violet and green lines indicate the confidence limits for $\alpha = 50\%$, 5% , and 1% respectively.

- Following Shebalin et al. (2011), the miss rates (v) of the analyzed models can also be compared to another **skilled reference model**, characterized by its space-time fractions occupied by alarms (τ_{ref}) and miss rates (v_{ref}).
- The miss rates (v_{ref}) of the **reference model** are plotted on the **diagonal line** of the Molchan diagram were $\tau = 1 - v_{ref}$.
- A **linear interpolation** is needed to plot the expected miss rates (v) of other models against $\tau = 1 - v_{ref}$, as they are computed at different values of τ compared to the reference model’s τ_{ref} .

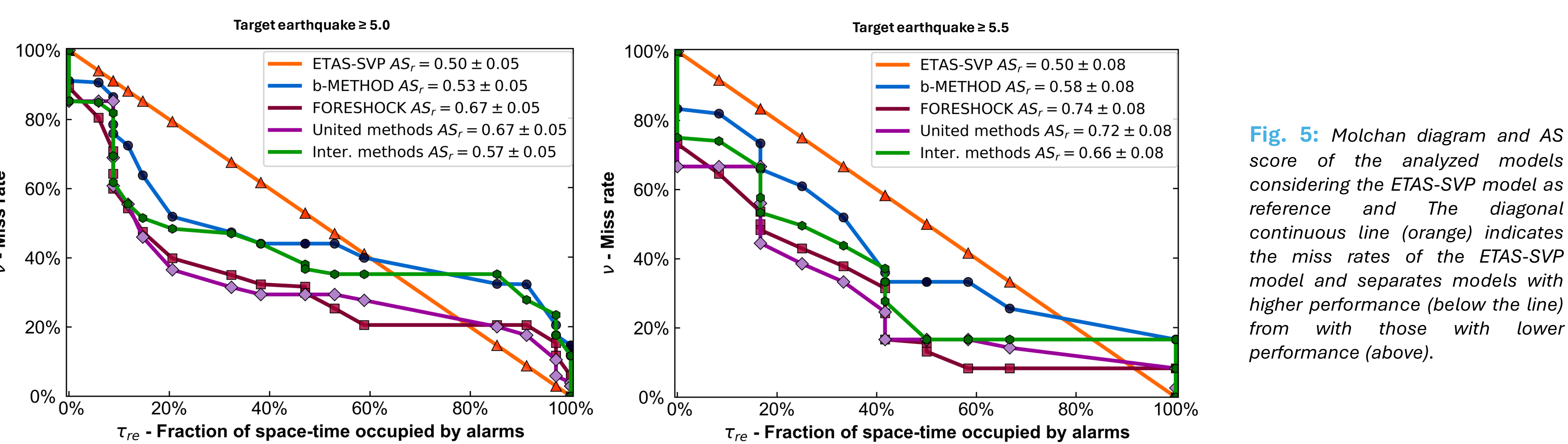


Fig. 5: Molchan diagram and AS score of the analyzed models considering the ETAS-SVP model as reference and The diagonal continuous line (orange) indicates the miss rates of the ETAS-SVP model and separates models with higher performance (below the line) from with those with lower performance (above).